

# Carbon release through abrupt permafrost thaw

Merritt R. Turetsky<sup>1,2\*</sup>, Benjamin W. Abbott<sup>3</sup>, Miriam C. Jones<sup>4</sup>, Katey Walter Anthony<sup>5</sup>, David Olefeldt<sup>6</sup>, Edward A. G. Schuur<sup>7</sup>, Guido Grosse<sup>8,9</sup>, Peter Kuhry<sup>10,11</sup>, Gustaf Hugelius<sup>10,11</sup>, Charles Koven<sup>12</sup>, David M. Lawrence<sup>13</sup>, Carolyn Gibson<sup>1</sup>, A. Britta K. Sannel<sup>10,11</sup> and A. David McGuire<sup>14</sup>

**The permafrost zone is expected to be a substantial carbon source to the atmosphere, yet large-scale models currently only simulate gradual changes in seasonally thawed soil. Abrupt thaw will probably occur in <20% of the permafrost zone but could affect half of permafrost carbon through collapsing ground, rapid erosion and landslides. Here, we synthesize the best available information and develop inventory models to simulate abrupt thaw impacts on permafrost carbon balance. Emissions across 2.5 million km<sup>2</sup> of abrupt thaw could provide a similar climate feedback as gradual thaw emissions from the entire 18 million km<sup>2</sup> permafrost region under the warming projection of Representative Concentration Pathway 8.5. While models forecast that gradual thaw may lead to net ecosystem carbon uptake under projections of Representative Concentration Pathway 4.5, abrupt thaw emissions are likely to offset this potential carbon sink. Active hillslope erosional features will occupy 3% of abrupt thaw terrain by 2300 but emit one-third of abrupt thaw carbon losses. Thaw lakes and wetlands are methane hot spots but their carbon release is partially offset by slowly regrowing vegetation. After considering abrupt thaw stabilization, lake drainage and soil carbon uptake by vegetation regrowth, we conclude that models considering only gradual permafrost thaw are substantially underestimating carbon emissions from thawing permafrost.**

Permafrost region soils store ~60% of the world's soil carbon in 15% of the global soil area<sup>1–3</sup>. Current estimates report 1,000 ± 150 PgC in the upper 3 m of active layer and permafrost soils (hereafter, permafrost carbon) and around another 500 PgC in deeper yedoma and deltaic deposits<sup>1,3,4</sup>. Rapid warming at high latitudes is causing accelerated decomposition of this permafrost carbon, releasing greenhouse gases into the atmosphere<sup>5</sup>. Initial studies suggested that permafrost carbon emissions could be large enough to create substantial impacts on the climate system<sup>6–8</sup>. More recently, an intercomparison of permafrost carbon-enabled models found a wide diversity of projections ranging from net carbon uptake from the atmosphere to large carbon releases from the permafrost region<sup>2,9</sup>. Despite uncertainties such as future biomass production offsets, models consistently predict that permafrost carbon is vulnerable to thaw and resulting emissions are likely to be substantial enough to merit consideration in emissions negotiations<sup>1,2,9–13</sup>.

The current frameworks of Earth system models applied to the northern permafrost region have focused primarily on how warming increases the thickness and changes the hydrological state of the seasonally thawed active layer<sup>11</sup>. As the high latitudes warm, vertical thickening of the active layer will occur gradually across much of the 18 million km<sup>2</sup> of permafrost soils. However, in areas with excess ground ice, surface subsidence called thermokarst can occur during permafrost degradation. Abrupt thaw processes such as thermokarst have long been recognized as influential but are complex and understudied, and thus are insufficiently represented in coupled models<sup>14</sup>. While gradual thaw slowly affects soil by centimetres over

decades, abrupt thaw can affect many metres of permafrost soil in periods of days to several years<sup>15</sup>.

In upland areas, abrupt thaw occurs as thaw slumps, gullies and active layer detachments, while in poorly drained areas abrupt thaw creates collapse scar wetlands and thermokarst lakes<sup>14</sup>. Across this range of landforms, abrupt thaw typically changes the hydrological state of permafrost material, either through downslope transport or in situ inundation or draining<sup>16</sup>. If thawed (formerly permafrost) material is exposed to saturated conditions, rates of carbon mineralization become limited by anoxia, but the proportion of CH<sub>4</sub> production increases. The carbon balance also changes as abrupt thaw features stabilize and undergo ecological succession (for example, as thermokarst lakes transition from large sources of atmospheric carbon when they initially form to eventual carbon sinks over millennial time scales)<sup>17–19</sup>.

## Data synthesis and first-order models

We recently described a Permafrost Carbon Network activity to synthesize observations in order to provide an initial estimate of the magnitude of abrupt thaw carbon emissions<sup>20</sup>. Here, we describe the numerical, inventory models of initial thaw and ecosystem recovery and present details of the first-order estimates of abrupt thaw carbon release. The goal of our study was to compare the magnitude of emissions from abrupt thaw relative to gradual thaw under similar model conditions. To achieve this, we developed a simple, unified framework for exploring ecosystem carbon balance across a diverse set of abrupt thaw processes. Our first-order inventory method is

<sup>1</sup>Department of Integrative Biology, University of Guelph, Guelph, Ontario, Canada. <sup>2</sup>Institute of Arctic and Alpine Research (INSTAAR), University of Colorado Boulder, Boulder, CO, USA. <sup>3</sup>Department of Plant and Wildlife Sciences, Brigham Young University, Provo, UT, USA. <sup>4</sup>United States Geological Survey, Reston, VA, USA. <sup>5</sup>Water and Environmental Research Center, University of Alaska, Fairbanks, AK, USA. <sup>6</sup>Department of Renewable Resources, University of Alberta, Edmonton, Alberta, Canada. <sup>7</sup>Center for Ecosystem Science and Society and Department of Biological Sciences, Northern Arizona University, Flagstaff, AZ, USA. <sup>8</sup>Alfred Wegener Institute Helmholtz Centre for Polar and Marine Research, Potsdam, Germany. <sup>9</sup>Institute of Geosciences, University of Potsdam, Potsdam, Germany. <sup>10</sup>Department of Physical Geography, Stockholm University, Stockholm, Sweden. <sup>11</sup>Bolin Centre for Climate Research, Stockholm University, Stockholm, Sweden. <sup>12</sup>Climate and Ecosystem Sciences Division, Lawrence Berkeley National Laboratory, Berkeley, CA, USA. <sup>13</sup>National Center for Atmospheric Research, Boulder, CO, USA. <sup>14</sup>Institute of Arctic Biology, University of Alaska Fairbanks, Fairbanks, AK, USA.

\*e-mail: [merritt.turetsky@colorado.edu](mailto:merritt.turetsky@colorado.edu)

similar to initial assessments of land-use carbon emissions<sup>21</sup>, and was used to simulate changes in ecosystem carbon balance during the initial abrupt thaw stage, as well as longer-term ecosystem recovery (Fig. 1).

### Abrupt thaw extent and carbon release

During the period 2000–2300, the area of abrupt thaw increased threefold under Representative Concentration Pathway 8.5 (RCP8.5) emissions and climate warming projection. Our historical assessment from 1900–2000 allows us to differentiate the impacts of background abrupt thaw from the accelerated thaw rates that could occur due to climate change. Our approach thus recognizes that abrupt thaw is a natural part of cyclical aggradation and degradation of ice-rich permafrost<sup>22</sup>. Abrupt thaw rates were known to be fast in the early Holocene, at least for thermokarst lakes<sup>17</sup>, but probably occurred under a lower temperature threshold than they do now. Despite this, studies clearly show that modern climate change is contributing to rapid increases in thaw rates<sup>23–25</sup>. At the start of the historical assessment in 1900, abrupt thaw affected 905,000 km<sup>2</sup> (~5% of the entire permafrost region). With warming and associated thaw, the total area of abrupt thaw increased to 1.6 million km<sup>2</sup> by 2100 and 2.5 million km<sup>2</sup> by 2300, while undisturbed permafrost vulnerable to abrupt thaw covered 1.5 million km<sup>2</sup> and 620,000 km<sup>2</sup> by 2100 and 2300, respectively. Increases in abrupt thaw area were driven by the initiation and expansion of newly formed active features that transitioned over time into more mature features that stabilized, potentially allowing permafrost to form again.

Increases in abrupt thaw due to climate warming triggered a change in carbon behaviour from net uptake to net release. Our simulations suggest net cumulative abrupt thaw carbon emissions on the order of  $80 \pm 19$  PgC by 2300 (Fig. 2a). For context, a recent modelling study found that gradual vertical thaw could result in permafrost carbon losses of 208 PgC by 2300 under RCP8.5 (multi-model mean), although model projections ranged from a net carbon gain of 167 PgC to a net loss of 641 PgC (ref. <sup>2</sup>). Thus, our results suggest that abrupt thaw carbon losses are equivalent to approximately 40% of the mean net emissions attributed to gradual thaw. Most of this carbon release stems from newly formed features that cover <5% of the permafrost region.

Our results corroborate previous studies showing that new thaw lakes function as a large regional carbon source to the atmosphere, but that lower and even net negative emissions are associated with older thaw lakes and drained lake basins<sup>17,22</sup>. When we allowed new thaw lakes to mature and eventually drain, the predicted area of new thaw lakes and their associated carbon emissions were both lower by 50% compared with simulations without lake maturation and drainage. The regrowth of vegetation in drained lake basins also partially offset permafrost carbon release from new thaw lakes (Fig. 2c). We conducted simulations with and without biomass gains during abrupt thaw stabilization and found that regrowing vegetation reduces total carbon emissions by ~20%, offsetting permafrost carbon release by 51 TgCyr<sup>-1</sup> on average from 2000–2300 (2000–2100: 36 TgCyr<sup>-1</sup>; 2100–2300: 58 TgCyr<sup>-1</sup>). Most of this biomass offset (85%) occurs in stabilized thaw lakes and wetlands.

From 2000–2300, newly formed hillslope erosional features increase in area from 0.1–3% of abrupt thaw terrain, but these active features have the potential to emit around one-third of abrupt thaw carbon losses (Fig. 2b). Our synthesis of published studies suggests that abrupt thaw carbon losses in these upland features are enhanced by three factors. First, microbial CO<sub>2</sub> production and permafrost carbon loss are stimulated by well-drained, oxic conditions<sup>26</sup>. Second, large amounts of permafrost carbon are vulnerable to rapid mineralization during erosion and downslope transport before reburial or fluvial export<sup>27,28</sup>. Finally, our simulations showed that recovering vegetation in these settings does little to replace losses of soil carbon after thaw.

While CH<sub>4</sub> accounted for only ~20% of carbon emissions, because of its strong atmospheric radiative forcing, it constituted 50% of the radiative forcing from abrupt thaw. Considering CO<sub>2</sub> and CH<sub>4</sub> emissions together, gradual thaw emissions ranged from 613–802 TgCO<sub>2</sub>eyr<sup>-1</sup> from 2000–2100<sup>12</sup>. During the same time period, our simulations showed that abrupt thaw could release 624 TgCO<sub>2</sub>eyr<sup>-1</sup>, increasing to 960 TgCO<sub>2</sub>eyr<sup>-1</sup> from 2100–2300. Thus, emissions from 2.5 million km<sup>2</sup> of abrupt thaw-impacted land could provide a similar positive feedback to climate warming as emissions associated with gradual thaw across the 18 million km<sup>2</sup> permafrost region. The contribution of CH<sub>4</sub> to abrupt thaw radiative forcing declined after 2100 due to lake drainage and drying associated with warming<sup>29</sup> (Fig. 2a,c,d). However, sustained CH<sub>4</sub> emissions from thaw wetlands were attributed to the increasing area over time of flowthrough fens (Fig. 2d).

Multiple lines of evidence suggest reduced gradual thaw permafrost carbon losses under an RCP4.5 climate<sup>2,10,12,30,31</sup> and our results corroborated this finding across different types of abrupt thaw. Overall, thaw lake emissions were relatively more important to the permafrost carbon feedback under RCP4.5 than RCP8.5 due to the lower level of gradual thaw emissions associated with RCP4.5, but also because earlier and stronger lake drainage dampened total lake emissions under RCP8.5 warming<sup>18</sup>. The results of our inventory model suggested that more aggressive climate change mitigation could reduce abrupt thaw carbon losses by ~50% relative to an RCP8.5 projection (reductions of 9 and 42 PgC by 2100 and 2300, respectively; Supplementary Table 5). Large-scale models of gradual permafrost thaw show the potential for net ecosystem carbon uptake under an RCP4.5 projection<sup>2</sup>. Most simulations using RCP4.5 projections forecast that the cumulative sink capacity of the northern permafrost region will remain under 50 PgC by 2300<sup>2</sup>. Under RCP4.5 climate, our results suggest that abrupt thaw will lead to carbon losses substantial enough to fully offset this enhanced sink capacity associated with gradual permafrost thaw.

As abrupt thaw is not simulated in any Earth system model, it remains an unresolved Earth system feedback to climate change from a climate policy perspective<sup>32</sup>. Our results suggest that abrupt thaw over the twenty-first century will lead to a CO<sub>2</sub> feedback of 3.1 PgC per °C global temperature increase and a CH<sub>4</sub> feedback of 1,180 TgC per °C global temperature increase under RCP8.5. Over the longer period to 2300, we estimate abrupt thaw feedbacks of 7.2 PgC CO<sub>2</sub> per °C increase and 1,970 TgC CH<sub>4</sub> per °C increase. These estimates suggest that the CO<sub>2</sub> feedback from abrupt thaw is modest but strengthens beyond the twenty-first century. In contrast, our estimates of the abrupt thaw CH<sub>4</sub> feedback are more substantial and vary less over time due to the balance between expanding thaw areas versus wetland and lake drying with continued warming. Interestingly, more aggressive climate change mitigation under RCP4.5 results in CO<sub>2</sub> feedbacks that are weaker in the short term but stronger in the long term, relative to the RCP8.5 projection: over the twenty-first century, the RCP4.5 CO<sub>2</sub> feedback from abrupt thaw is 2.3 PgC per °C increase, but increases to 11.6 PgC per °C increase beyond the twenty-first century. The RCP4.5 abrupt thaw CH<sub>4</sub> feedback (2,330 TgC CH<sub>4</sub> per °C increase during the twenty-first century, increasing to 5,605 TgC CH<sub>4</sub> per °C through 2300) is stronger at both time scales than the RCP8.5 feedback. These changes in the sensitivity of the abrupt thaw feedback, both over time and in response to different warming scenarios, point to a limitation of the linear feedback framework for quantifying the warming from these processes.

The development of mechanistic representations of these processes will require a deeper understanding of the processes that control these fine-scale features and how to represent them in coarser-scale global models. For now, we advocate considering abrupt thaw processes within the set of Earth system model-unresolved

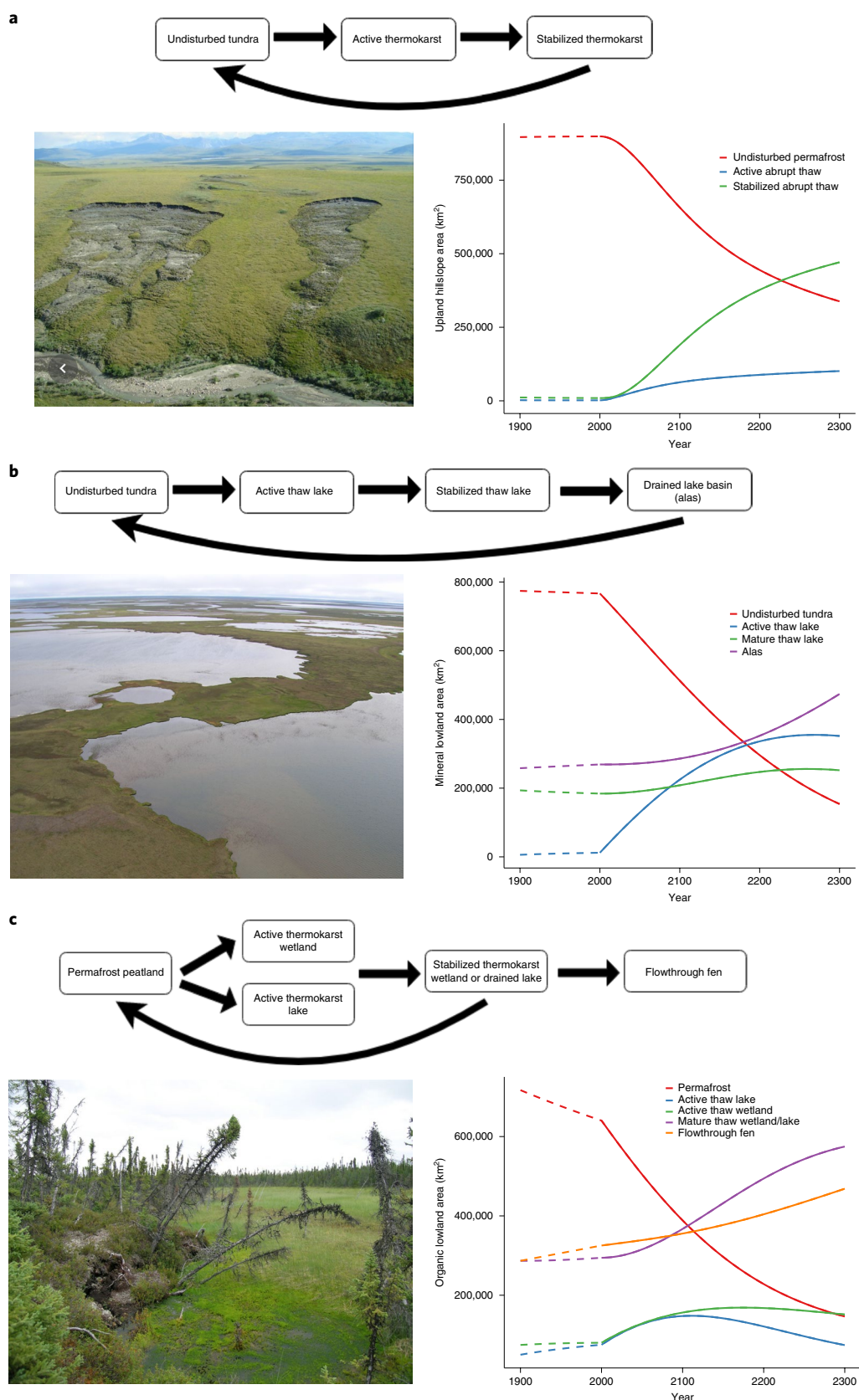


**Fig. 1 | Models of abrupt thaw succession. a–c.** Pathways of ecosystem succession and changes with simulated abrupt thaw formation and stabilization in: hillslope/upland landscapes where abrupt thaw leads to slumps, active layer detachments and gullies (**a**); lowland mineral landscapes with the formation of thaw lakes (**b**); and lowland organic landscapes with the formation of thaw lakes or wetlands (**c**). The assessment period between 1900 and 2000 (dashed lines) was based on historical transition rates between successional states. Between 2000 and 2300 (solid lines), the assessment simulates increasing permafrost thaw rates under RCP8.5 climate projection, as projected by large-scale models<sup>2</sup>.

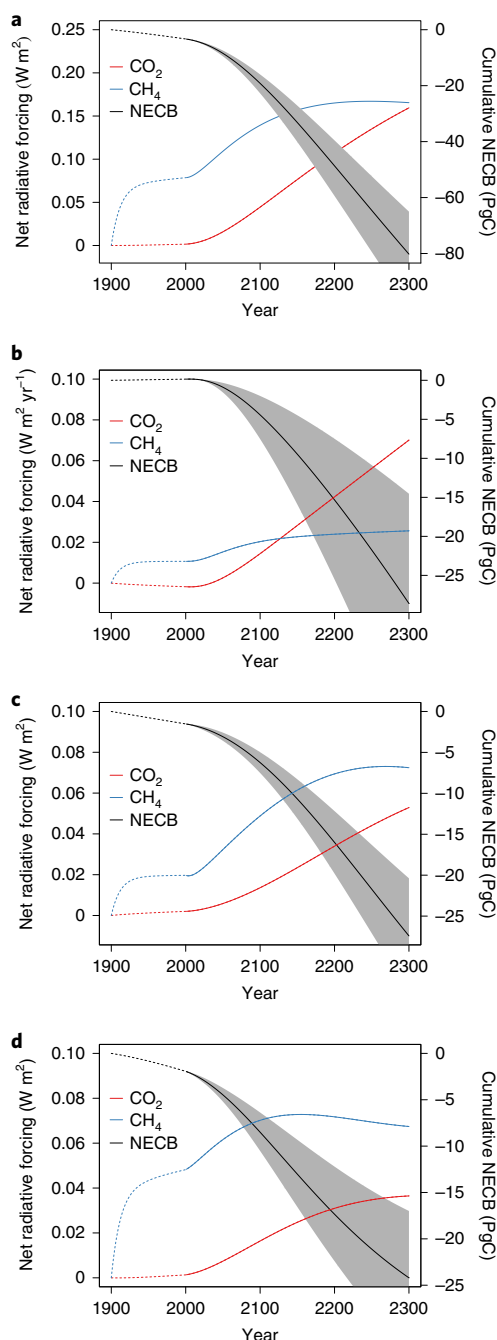


**Fig. 2 | Simulated carbon release due to abrupt thaw.** **a–d**, Simulated cumulative changes in net ecosystem carbon balance (NECB) (means  $\pm$  s.d.) and the radiative greenhouse gas forcing of  $\text{CO}_2$  relative to  $\text{CH}_4$  for: total abrupt thaw across the permafrost region (**a**); and abrupt thaw in hillslope landscapes leading to slumps, gullies or active layer detachments (**b**), lowland mineral landscapes leading to thermokarst lake formation (**c**) and lowland organic landscapes leading to thaw wetland or lake formation (**d**). Positive NECB values represent ecosystem carbon uptake, whereas negative values represent ecosystem carbon loss. Radiative forcing data are cumulative values, whereby positive forcing denotes incoming energy exceeding outgoing energy.

feedbacks for the purposes of climate policy<sup>32</sup>, in the same way that models are beginning to include biogeochemical responses to widespread gradual permafrost thaw.

### Key assumptions and caveats

The main goal of this study was to assess how abrupt thaw emissions compare with those estimated for widespread gradual thaw, under similar modelling conditions and warming scenarios<sup>2</sup>. We achieved this by assuming that abrupt thaw rates will increase similarly to gradual thaw rates with climate change as predicted by large-scale models<sup>2</sup>. We recognize that this assumption is a substantial simplification, but at this point we do not know whether this assumption would over- or underestimate abrupt thaw expansion. This is an important knowledge gap because the sensitivity of gradual thaw to climate change may not be the same as abrupt thaw, which can be triggered by a single weather extreme<sup>23,33</sup>. In addition, once initiated, abrupt thaw features can evolve with self-reinforcing feedbacks such as continued thaw subsidence with increasing water depth and volume in the case of lakes and with changes in vegetation and albedo in thaw wetlands<sup>34,35</sup>. These feedbacks cause abrupt thaw to become less dependent on external climate after initiation, as indicated by the presence of actively expanding thaw lakes even in High Arctic cold permafrost regions today<sup>23–25,36</sup>.

Our inventory model focused on ecosystem carbon changes and did not track modern versus older sources of carbon emissions. As models improve their mechanistic representation of abrupt thaw, information on  $^{14}\text{C}$   $\text{CH}_4$  and  $^{14}\text{C}$   $\text{CO}_2$  released from abrupt thaw features could help to constrain total ecosystem carbon losses. Carbon released from abrupt thaw features reflects the net result of several biophysical processes that vary in isotopic composition, including: (1) inundation with lake/wetland expansion; (2) release of geological  $\text{CH}_4$  (typically fossil;  $^{14}\text{C}$   $\text{CH}_4$ ), which is known to escape in relatively huge quantities from a very small number of thermokarst lakes; and (3) microbial decomposition of thawed permafrost soil organic matter at depth, resulting in carbon emissions reflecting the age of the thawing permafrost soils<sup>37</sup>. Information on the relative contributions of these processes to ecosystem carbon balance would also improve our understanding of the role of abrupt thaw in past climate, given ongoing debates about sources of the rise in atmospheric  $\text{CH}_4$  at the end of the last glacial maximum<sup>38,39</sup>.

Our simulations do not include dynamic vegetation changes expected in high-latitude regions with warming. We note that large-scale models do not include vegetation dynamics associated with thermokarst, making our state-based approach complementary to previous studies. More generally, while some global dynamic vegetation models simulate rapid northern treeline advancement, process-based regional modelling studies tend to show much slower migration of trees northward<sup>40</sup>. For both gradual and abrupt permafrost thaw, large-scale models will need to more realistically simulate time lags in tree dispersal and colonization. Finally, our inventory approach also does not account for potential biomass enhancements in response to climate change. Given that large-scale gradual thaw models show that the strength of  $\text{CO}_2$  fertilization in combination with vegetation response to climate can dictate the sign of the overall net carbon balance<sup>2</sup>, this is an important topic for future research with respect to abrupt thaw. In contrast, given that abrupt thaw affects small areas within the permafrost region, it is possible that the details of the vegetation response will not be as important in determining abrupt thaw emissions as they are to widespread gradual thaw emissions.

We believe the first-order abrupt thaw estimates presented here are valid but probably conservative. For example, we only apply our successional models to the 3.6 million  $\text{km}^2$  portion of the permafrost region that is classified as being vulnerable to abrupt thaw<sup>14</sup>, thereby excluding a large proportion of the northern permafrost region that is thought to contain low-ice-content permafrost or other geomorphic factors that may not favour abrupt thaw. Despite our conservative approach, we found that a very small fraction of the northern permafrost region can contribute up to 40% additional permafrost



carbon release and increase overall global warming potential by approximately 100%.

Our synthesis of abrupt thaw studies identified several additional important knowledge gaps that will require additional research before abrupt thaw emissions can be mechanistically simulated. Below, we explore the sensitivity of our results to these issues.

### Predicting future thaw lake area

A model simulating talik development and expansion beneath thermokarst lakes across the entire 18 million km<sup>2</sup> permafrost region predicts that new lake formation will peak at approximately 1 million km<sup>2</sup> by 2100 under an RCP8.5 climate<sup>18,19</sup>. Our synthesis and upscaling focused on the 3.6 million km<sup>2</sup> considered to be predisposed to abrupt thaw, and suggests that new thaw lake area under an RCP8.5 projection will peak just over 200,000 km<sup>2</sup>. When we entirely disable post-thaw succession in our simulations, new thaw lakes in lowland mineral and organic permafrost regions expand to cover 545,000 km<sup>2</sup> by 2100 and 1,048,000 km<sup>2</sup> by 2300. Such an increase in simulated lake area would result in a doubling of thaw lake carbon emissions to 60 PgC by 2300. This suggests that discrepancies between modelled thaw lake emissions (refs. <sup>18,19</sup> and our results) can largely be attributed to how the models are projecting new thaw lake areas in the future. High-resolution Landsat-based remote sensing observations of recent thaw lake dynamics (1999–2014) across a large 2.3 million km<sup>2</sup> proportion (~10%) of the permafrost domain suggests highly variable lake trajectories<sup>41</sup>. Understanding spatial patterns plus relationships between warming and northern hydrology (for example, evaporation, lake ice and talik dynamics, groundwater connections and runoff) will be critical for predicting future thaw lake area and behaviour.

### Fate of thaw-induced erosion

The main scenario used in our simulations was based on starting thaw rates bound by historical observations of abrupt thaw expansion rates (Supplementary Information). Several recent studies suggest that ongoing hillslope thaw is exceeding these historical bounds<sup>23–25,36</sup>. The dependency of hillslope abrupt thaw on slope and preferential flow paths leads to constraints on their areal extent, which is complex<sup>42,43</sup>, but which could provide a pathway forward to upscaling and simulation. These spatial constraints were considered in the initial areas used in our simulations, as hillslope abrupt thaw predisposition classes were assigned more stringently than lake or wetland thaw classes<sup>14</sup>. In any individual region, no more than 40% of the landscape was predisposed to hillslope abrupt thaw<sup>14</sup> and this was factored into the initial areas we used as model inputs. At the start of our simulations, active or stabilized abrupt thaw features affected <2% of the total area predisposed to hillslope abrupt thaw. Over time, abrupt thaw areas increased under the warming scenario but did not exceed 60% of the area predisposed to hillslope abrupt thaw. Thus, by 2300, no more than 24% of the landscape in any region (0.4 × 0.6) could experience hillslope abrupt thaw in our study.

### Peat history regulates permafrost carbon loss

In organic soil-rich regions, studies tend to show loss of soil carbon either during active layer thickening<sup>44</sup> or during the early stages of thaw wetland formation<sup>45,46</sup>. The magnitude of soil carbon loss during or soon after thaw appears to depend on permafrost formation processes or the degree of peat decomposition that occurred before peat being incorporated into what ultimately became permafrost soil horizons<sup>22,46</sup>. Here, we capture some of this complexity by including carbon stock changes from both epigenetic and syngenetic permafrost peatland sites (Supplementary Methods), but information from a wider range of permafrost and peat conditions is required so that these transformations can be more fully understood and better represented in large-scale models.

### Online content

Any methods, additional references, Nature Research reporting summaries, source data, extended data, supplementary information, acknowledgements, peer review information; details of author contributions and competing interests; and statements of data and code availability are available at <https://doi.org/10.1038/s41561-019-0526-0>.

Received: 26 March 2019; Accepted: 16 December 2019;

Published online: 3 February 2020

### References

- Schuur, E. A. G. et al. Climate change and the permafrost carbon feedback. *Nature* **520**, 171–179 (2015).
- McGuire, A. D. et al. Dependence of the evolution of carbon dynamics in the northern permafrost region on the trajectory of climate change. *Proc. Natl Acad. Sci. USA* **115**, 3882–3887 (2018).
- Hugelius, G. et al. Estimated stocks of circumpolar permafrost carbon with quantified uncertainty ranges and identified data gaps. *Biogeosciences* **11**, 6573–6593 (2014).
- Schuur, E. A. G., McGuire, A. D., Romanovsky, V., Schädel, C. & Mack, M. in *Second State of the Carbon Cycle Report (SOCCR2): A Sustained Assessment Report* (eds Cavallaro, N. et al.) 428–468 (US Global Change Research Program, 2018).
- Schuur, E. A. G. et al. Vulnerability of permafrost carbon to climate change: implications for the global carbon cycle. *Bioscience* **58**, 701–714 (2008).
- Khvorostyanov, D. V. et al. Vulnerability of permafrost carbon to global warming. Part II: sensitivity of permafrost carbon stock to global warming. *Tellus B Chem. Phys. Meteorol.* **60**, 265–275 (2007).
- Tarnocai, C. The effect of climate warming on the carbon balance of cryosols in Canada. *Permafrost Periglac. Process.* **10**, 251–263 (1999).
- Zimov, S. A. et al. Permafrost carbon: stock and decomposability of a globally significant carbon pool. *Geophys. Res. Lett.* **33**, L20502 (2006).
- Schaefer, K., Lantuit, H., Romanovsky, V. E., Schuur, E. A. G. & Witt, R. The impact of the permafrost carbon feedback on global climate. *Environ. Res. Lett.* **9**, 085003 (2014).
- Abbott, B. W. et al. Biomass offsets little or none of permafrost carbon release from soils, streams, and wildfire: an expert assessment. *Environ. Res. Lett.* **11**, 034014 (2016).
- Lawrence, D. M., Koven, C. D., Swenson, S. C., Riley, W. J. & Slater, A. G. Permafrost thaw and resulting soil moisture changes regulate projected high-latitude CO<sub>2</sub> and CH<sub>4</sub> emissions. *Environ. Res. Lett.* **10**, 094011 (2015).
- Koven, C. D. et al. A simplified, data-constrained approach to estimate the permafrost carbon–climate feedback. *Phil. Trans. R. Soc. A Math. Phys. Eng. Sci.* **373**, 20140423 (2015).
- MacDougall, A. H., Avis, C. A. & Weaver, A. J. Significant existing commitment to warming from the permafrost carbon feedback. *Nat. Geosci.* **5**, 719–721 (2012).
- Olefeldt, D. et al. Circumpolar distribution and carbon storage of thermokarst landscapes. *Nat. Commun.* **7**, 13043 (2016).
- Grosse, G. et al. Vulnerability of high-latitude soil organic carbon in North America to disturbance. *J. Geophys. Res.* **116**, G00K06 (2011).
- Kokelj, S. V. & Jorgenson, M. T. Advances in thermokarst research. *Permafrost Periglac. Process.* **24**, 108–119 (2013).
- Walter Anthony, K. M. et al. A shift of thermokarst lakes from carbon sources to sinks during the holocene epoch. *Nature* **511**, 452–456 (2014).
- Walter Anthony, K. M. et al. 21st-century modeled permafrost carbon emissions accelerated by abrupt thaw beneath lakes. *Nat. Commun.* **9**, 3262 (2018).
- Schneider von Deimling, T. et al. Observation-based modelling of permafrost carbon fluxes with accounting for deep carbon deposits and thermokarst activity. *Biogeosciences* **12**, 3469–3488 (2015).
- Turetsky, M. R. et al. Permafrost collapse is accelerating carbon release. *Nature* **569**, 32–34 (2019).
- Houghton, R. A. et al. Changes in the carbon content of terrestrial biota and soils between 1860–1980. *Ecol. Monogr.* **53**, 235–262 (1983).
- Treat, C. C. et al. Effects of permafrost aggradation on peat properties as determined from a pan-Arctic synthesis of plant macrofossils. *J. Geophys. Res.* **121**, 78–94 (2016).
- Lewkowicz, A. G. & Way, R. G. Extremes of summer climate trigger thousands of thermokarst landslides in a High Arctic environment. *Nat. Commun.* **10**, 1329 (2019).
- Jones, M. K. W., Pollard, W. H. & Jones, B. M. Rapid initialization of retrogressive thaw slumps in the Canadian High Arctic and their response to climate and terrain factors. *Environ. Res. Lett.* **14**, 055006 (2019).
- Farquharson, L. M. et al. Climate change drives widespread and rapid thermokarst development in very cold permafrost in the Canadian High Arctic. *Geophys. Res. Lett.* **46**, 6681–6689 (2019).

26. Schädel, C. et al. Potential carbon emissions dominated by carbon dioxide from thawed permafrost soils. *Nat. Clim. Change* **6**, 950–953 (2016).
27. Serikova, S. et al. High riverine CO<sub>2</sub> emissions at the permafrost boundary of western Siberia. *Nat. Geosci.* **11**, 825–829 (2018).
28. Vonk, J. E. et al. High biolability of ancient permafrost carbon upon thaw. *Geophys. Res. Lett.* **40**, 2689–2693 (2013).
29. Sannel, A. B. K. & Kuhry, P. Warming-induced destabilization of peat plateau/thermokarst lake complexes. *J. Geophys. Res.* **116**, G03035 (2011).
30. Schuur, E. A. G. et al. Expert assessment of vulnerability of permafrost carbon to climate change. *Clim. Change* **119**, 359–374 (2013).
31. Kleinen, T. & Brovkin, V. Pathway-dependent fate of permafrost region carbon. *Environ. Res. Lett.* **13**, 094001 (2018).
32. Rogelj, J. et al. in *Special Report on Global Warming of 1.5 °C* (eds Masson-Delmotte, V. et al.) 93–174 (WMO, 2018).
33. Balser, A. W., Jones, J. B. & Gens, R. Timing of retrogressive thaw slump initiation in the Noatak Basin, northwest Alaska, USA. *J. Geophys. Res.* **119**, 1106–1120 (2014).
34. Lorant, M. M. et al. Reviews and syntheses: changing ecosystem influences on soil thermal regimes in northern high-latitude permafrost regions. *Biogeosciences* **15**, 5287–5313 (2018).
35. Baltzer, J. L., Veness, T., Chasmer, L. E., Sniderhan, A. E. & Quinton, W. L. Forests on thawing permafrost: fragmentation, edge effects, and net forest loss. *Glob. Change Biol.* **20**, 824–834 (2014).
36. Kokelj, S. V., Lantz, T. C., Tunnicliffe, J., Segal, R. & Lacelle, D. Climate-driven thaw of permafrost preserved glacial landscapes, northwestern Canada. *Geology* **45**, 371–374 (2017).
37. Walter Anthony, K. M. et al. Methane emissions proportional to permafrost carbon thawed in arctic lakes since the 1950s. *Nat. Geosci.* **9**, 679–682 (2016).
38. Petrenko, V. et al. Minimal geological methane emissions during the younger dryas–preboreal abrupt warming event. *Nature* **548**, 443–446 (2017).
39. Beck, J. et al. Bipolar carbon and hydrogen isotope constraints on the Holocene methane budget. *Biogeosciences* **15**, 7155–7175 (2018).
40. Kruse, S. et al. Dispersal distances and migration rates at the arctic treeline in Siberia—a genetic and simulation-based study. *Biogeosciences* **16**, 1211–1224 (2019).
41. Nitze, I., Grosse, G., Jones, B. M., Romanovsky, V. E. & Boike, J. Remote sensing quantifies widespread abundance of permafrost region disturbances across the Arctic and Subarctic. *Nat. Commun.* **9**, 5423 (2018).
42. Abbott, B. W., Jones, J. B., Godsey, S. E., Larouche, J. R. & Bowden, W. B. Patterns and persistence of hydrologic carbon and nutrient export from collapsing upland permafrost. *Biogeosciences* **12**, 3725–3740 (2015).
43. Tanski, G. et al. Transformation of terrestrial organic matter along thermokarst-affected permafrost coasts in the Arctic. *Sci. Total Environ.* **581–582**, 434–447 (2017).
44. Estop-Aragones, C. et al. Respiration of aged soil carbon during fall in permafrost peatlands enhanced by active layer deepening following wildfire but limited following thermokarst. *Environ. Res. Lett.* **13**, 085002 (2018).
45. O'Donnell, J. A. et al. The effects of permafrost thaw on soil hydrologic, thermal, and carbon dynamics in an Alaskan peatland. *Ecosystems* **15**, 213–229 (2012).
46. Jones, M. C. et al. Rapid carbon loss and slow recovery following permafrost thaw in boreal peatlands. *Glob. Change Biol.* **23**, 1109–1127 (2017).

**Publisher's note** Springer Nature remains neutral with regard to jurisdictional claims in published maps and institutional affiliations.

© The Author(s), under exclusive licence to Springer Nature Limited 2020

## Methods

**Abrupt thaw data synthesis.** This study considers three generalized types of abrupt thaw: (1) upland terrain in which abrupt thaw is typically expressed as hillslope erosional features such as thaw slumps, thermo-erosion gullies and active layer detachments; (2) lowland mineral soil terrain in which abrupt thaw leads primarily to thermokarst lake formation; and (3) lowland organic soil terrain in which abrupt thaw can lead to the creation of thermokarst lakes or collapse scar wetlands (Fig. 1 and Supplementary Methods). The total area of land associated with each abrupt thaw type is based on a spatial analysis of landscape predisposition to upland, lowland mineral and lowland organic abrupt thaw<sup>14</sup>. This was based on spatial analysis of key factors involved in abrupt thaw, such as topography and high ground-ice content, which showed that 3.6 million km<sup>2</sup>, or 20% of the northern permafrost region, is susceptible to future abrupt thaw or has already undergone abrupt thaw<sup>14</sup> (total area predisposed to upland abrupt thaw: 900,900 km<sup>2</sup>; lowland mineral abrupt thaw: 1,232,000 km<sup>2</sup>; lowland organic abrupt thaw: 1,434,000 km<sup>2</sup>). Within each abrupt thaw type, we synthesized recent change detection and remote sensing studies to determine the starting areas of undisturbed ice-rich permafrost as well as active versus stabilized abrupt thaw states.

To understand rates of transition from undisturbed permafrost to active abrupt thaw, we synthesized field observations and remote sensing measurements of recent thermokarst area expansion made throughout the circumpolar north over the past several decades. Remote sensing and palaeoecological studies were synthesized in order to understand the rates of transition between other ecosystem states (that is, from active to stabilized abrupt thaw features or the re-accumulation of permafrost within stabilized thaw features over time). The results of our synthesis activity represent our best understanding of the proportion of abrupt thaw that has been present in the northern permafrost region in the recent past, and our approach recognizes that some level of abrupt thaw activity has been a natural part of the cyclical aggradation and degradation of ice-rich permafrost.

Finally, we synthesized the literature on ecosystem carbon stocks and fluxes for each ecosystem state within each abrupt thaw type. Our synthesis focused on estimating the mean annual net ecosystem exchange of CO<sub>2</sub> (NEE), as well as the mean annual CH<sub>4</sub> emissions for each ecosystem state listed in the successional diagrams in Fig. 1. Losses of particulate and dissolved carbon into streams and lakes also were estimated for upland hillslope abrupt thaw. Positive values represent ecosystem carbon uptake while negative values represent ecosystem carbon loss.

The results of our data synthesis activity on starting ecosystem state areas, transition rates and carbon fluxes are reported in Supplementary Tables 1–4. Supporting details are included in the Supplementary Methods.

**Development of successional cycles and numerical inventory models.** We developed conceptual models simulating the initial and longer-term changes in post-abrupt thaw succession (Fig. 1). This framework is used to investigate abrupt thaw carbon release over a 300-year projection period compared with similar carbon release estimates focused on gradual thaw processes. All simulations were run using the R package FME<sup>47</sup>, which was designed to conduct comprehensive analyses including algorithms for inverse modelling with optimization methods, parameter identifiability analysis, and sensitivity and Monte Carlo analysis. Detailed information about the functions of FME is available from the R Archive Network at <https://cran.r-project.org/web/packages/FME/index.html>. In FME, we tracked changes in the area of each successional state (Fig. 1) over time by multiplying initial starting areas by appropriate transition rates. We tracked carbon fluxes over time by multiplying the spatial extent by annual carbon fluxes for each successional state. For example, the upland abrupt thaw model has three successional states based on our literature synthesis: undisturbed tundra, active abrupt thaw features that persist for 10 years on average and stabilized abrupt thaw features that persist for 60 years before transitioning back to undisturbed tundra (Supplementary Information). From this, the total change in hillslope abrupt thaw NECB can be calculated via the following steps:

1. Undisturbed net ecosystem carbon balance (NECB) =  $((-a \times \text{area undisturbed} + b \times \text{area stabilized}) \times (\text{undisturbed NEE} + \text{undisturbed CH}_4 + \text{undisturbed dissolved organic carbon flux export (DOC)}))$
2. Active thaw NECB =  $((a \times \text{area undisturbed} - c \times \text{area active}) \times (\text{active NEE} + \text{active CH}_4 + \text{active DOC}))$
3. Stabilized thaw NECB =  $((c \times \text{area young} - b \times \text{area stabilized}) \times (\text{stabilized NEE} + \text{stabilized CH}_4 + \text{stabilized DOC}))$
4. Total change in hillslope abrupt thaw NECB = annual change in undisturbed NECB + annual change in active thaw NECB + annual change in stabilized thaw NECB

where  $a$  is the abrupt thaw rate or the transition from undisturbed tundra to active abrupt thaw feature,  $b$  is the transition rate of stabilized abrupt thaw feature to undisturbed tundra and  $c$  is the transition rate of active to stabilized abrupt thaw feature. Transition rates are the reciprocal of the lifetime (years of persistence) of each abrupt thaw state. Source data for all model inputs are provided in the Supplementary Methods. In our simulations, carbon flux data are inputted to the model in gC m<sup>-2</sup> yr<sup>-1</sup> and we present output as NECB across the abrupt thaw terrain in PgC yr<sup>-1</sup>.

Rather than directly forcing our conceptual models with temperature changes projected by climate model simulations for different RCP projections, we represent the outcome of warming by increasing rates of abrupt thaw through time. We achieved this by adjusting the permafrost thaw rate (the rate at which undisturbed permafrost has transitioned to an active thaw state in the recent past) to increase during the projection period (Supplementary Tables 1–3). This increase in thaw rate was prescribed to follow the average output of ‘permafrost-enabled’ land-surface models, all of which were forced by atmospheric climate anomalies from the Community Climate System Model 4 (CCSM4) Earth system model under an RCP8.5 projection<sup>2</sup> (Supplementary Figs. 2, 4 and 6). Transition rates reflecting lake drainage were also adjusted dynamically over time to reflect accelerated landscape drainage associated with warming, increased evapotranspiration, as well as increases in woody plant transpiration expected to occur at high latitudes in the future. We used a similar approach to simulate a more aggressive climate change mitigation pathway (that is, we prescribed thaw rates in our inventory model to follow the average output of ‘permafrost-enabled’ land-surface models forced by atmospheric climate anomalies from the CCSM4 Earth system model under an RCP4.5 projection)<sup>2</sup>. Thaw rates for both climate change projections are described in Supplementary Figs. 2, 4 and 6.

For a 300-year dynamic measurement period (2000–2300), we used our data synthesis along with the dynamic increases in transition rates over time to simulate the effects of RCP4.5 versus RCP8.5 climate warming on permafrost thaw and to investigate how increases in abrupt thaw rates affect NECB. We also included simulations for a 100-year historical measurement period (1900–2000). The goal of the historical measurement period was to provide an informal means of model spin up, mainly so that regional carbon fluxes did not start at zero at the beginning of the dynamic measurement period. Parameters in the historical model run were fitted so that abrupt thaw rates approximated an equilibrium with permafrost recovery at the regional scale. This allowed us to explore NECB at regional scales under these quasi-equilibrium conditions and then compare these values with changes in NECB under accelerated thaw rates in the dynamic measurement period. In most cases, the thaw rates used in the historical measurement period were slower than those obtained in our data synthesis and used for the start of the dynamic measurement period, reflecting the fact that many remote sensing and change detection studies over the past several decades have probably already documented the effects of climate change on abrupt thaw rates. We subtracted carbon emissions from 1900–2000 from our results and focused mainly on emissions from 2000–2300.

We compared our emission estimates with what has been published for gradual thaw using three approaches. First, we calculated emissions in the carbon equivalent by multiplying CH<sub>4</sub> carbon by a 100-year global warming potential of 34 (ref. 48), adjusting for the different molecular weights of CO<sub>2</sub> and CH<sub>4</sub> and summing the changes to the integrated CO<sub>2</sub> and CH<sub>4</sub> budgets over time. We used the 100-year global warming potential because it allows us to specify a discrete, societally relevant time scale over which to compare the differing effects of short-lived CH<sub>4</sub> and long-lived CO<sub>2</sub>. Second, we used a simple approach to quantify the instantaneous radiative forcing of CH<sub>4</sub> and CO<sub>2</sub> (refs. 49,50). In our calculations, CH<sub>4</sub> emitted to the atmosphere was treated as a single reservoir with annual input and a first-order loss (reservoir mass divided by constant reservoir lifetime or adjustment time). CO<sub>2</sub> was simulated as a collection of five non-interacting reservoirs with different reservoir lifetimes. The input of each reservoir was a fraction of the annual flux, and the loss was determined by reservoir lifetime. The separate radiative forcings of CH<sub>4</sub> and CO<sub>2</sub> were calculated annually by multiplying the reservoir mass by a constant radiative forcing factor for each gas. The total greenhouse gas radiative forcing was then calculated by summing the contributions of each individual gas. This approach is useful for comparing the behaviour of abrupt thaw CO<sub>2</sub> versus CH<sub>4</sub> emissions, but does not consider the dependency of radiative forcing on the trajectory of atmospheric CO<sub>2</sub> and CH<sub>4</sub> concentrations. Third, to consider these processes from a linearized climate feedback perspective, we calculated the mass-based carbon feedbacks per degree of warming stemming from abrupt thaw. These calculations relied on the CCSM4 surface air temperature fields (RCP8.5 and 4.5 projections), which were used in a recent comparison study of large-scale permafrost models<sup>5</sup>, with climate data from 1850–1950 as background for our calculations.

We estimated the local sensitivities of all input parameters using the FME sensFun function with initial parameter values and a relative change (that is, an increase of 10% of the initial value) as inputs. We used the magnitudes of the sensitivity summary values to rank the importance of parameters on the output variables. Variables with a sensitivity of zero were excluded from further quantification of carbon flux uncertainty. We implemented the sensRange function, using an assumed standard error of  $\pm 40\%$  for each parameter, to estimate the effect of this suite of parameter uncertainty identified in the local sensitivity analyses on the model output variables. For comparison, empirically measured errors for input parameters, which were often smaller than 40%, are summarized in Supplementary Tables 1–4.

We conducted two sets of model simulations to further explore controls on abrupt thaw carbon emissions. First, we explored the effects of lake maturation and drainage on NECB in the lowland organic and lowland mineral abrupt thaw submodels. In these simulations, we implemented the historical and dynamic thaw rate representing the transition between permafrost and young thaw lakes, but all other transitions were set to zero to prevent young thaw lakes from undergoing post-thaw succession and maturation. This simulation allowed us to compare our

results more directly with previous studies that focused on carbon release from new thaw lake growth and expansion<sup>17,18</sup>. We also conducted simulations in each of the abrupt thaw submodels to quantify the magnitude of carbon uptake from vegetation regrowth. In these simulations, we set carbon uptake associated with net primary productivity in stabilized hillslope features, mature collapse scar wetlands, mature thaw lakes and alas to zero. For these independent model simulations, we compared the resulting carbon emissions with the fluxes presented in Fig. 2 and the Supplementary Data.

### Data availability

All synthesized data used as model inputs, plus associated references, are provided in the Supplementary Data. Modelled data that support the findings of this study are also provided in the Supplementary Data.

### Code availability

RMD files containing full code for the three generalized abrupt thaw models are available at <https://github.com/mturetsky/Abrupt-thaw-carbon-model>.

### References

47. Soetaert, K. & Petzoldt, T. Inverse modeling, sensitivity, and Monte Carlo analysis in R using package FME. *J. Stat. Softw.* <https://doi.org/10.18637/jss.v033.i03> (2010)..
48. Myhre, G. et al. in *Climate Change 2013: The Physical Science Basis* (eds Stocker, T. F. et al.) 659–740 (Cambridge Univ. Press, 2013).
49. Frolking, S. & Roulet, N. T. Holocene radiative forcing impact of northern peatland carbon accumulation and methane emissions. *Glob. Change Biol.* **13**, 1079–1088 (2007).
50. Frolking, S., Roulet, N. & Fuglestad, J. How northern peatlands influence the Earth's radiative budget: sustained methane emission versus sustained carbon sequestration. *J. Geophys. Res.* **111**, G01008 (2006).

### Acknowledgements

S. Frolking provided guidance on the radiative forcing calculations. M. Strimas-Mackey and A. McAdam provided assistance with the R coding. T. Douglas provided constructive feedback on the manuscript. This work is a product of the Permafrost Carbon Network and SEARCH Permafrost Action Team. We acknowledge support from NSERC (to M.R.T.), the PETA-CARB project (ERC number 338335) and BMBF KoPf project (to G.G.), and NSF ARCSS 1500931 and NASA ABoVE (to K.W.A.).

### Author contributions

M.R.T. and A.D.M. conceived of the study. B.W.A., M.C.J., K.W.A. and M.R.T. led the development of each abrupt thaw conceptual model. G.G. and C.G. participated in remote sensing analysis and synthesis. M.R.T., G.G. and K.W.A. led the synthesis of thaw lake data. M.R.T., M.C.J., D.O. and A.B.K.S. led the synthesis of permafrost peatland data. G.G. led the synthesis of head wall retreat rates. B.W.A. and E.A.G.S. led the synthesis of hillslope data. M.R.T. performed the simulations and wrote the paper. All authors commented on the analysis, interpretation and presentation of the data and were involved with the writing.

### Competing interests

The authors declare no competing interests.

### Additional information

**Supplementary information** is available for this paper at <https://doi.org/10.1038/s41561-019-0526-0>.

**Correspondence and requests for materials** should be addressed to M.R.T.

**Peer review information** Primary Handling Editors: Xujia Jiang; Heike Langenberg.

**Reprints and permissions information** is available at [www.nature.com/reprints](http://www.nature.com/reprints).